InnoVationinfo

ISSN: 2581-7566

Volume 5: 1

Journal of Applied Microbiological Research

J Appl Microb Res 2022

In Vivo Monitoring of Viable Bacteria by SPECT using ^{99m}Tc-HYNIC(GH)$_2$-UBI 29-41 and ^{99m}Tc-HYNIC(Tricine)$_2$-UBI 29-41 in Infected Mice

Yuri Nishiyama[1*]
Tomoya Uehara[2]
Kenichi Okazaki[1]
Hideki Maki[1]
Kohji Abe[3]
Yasushi Arano[2]
Sotaro Momosaki[3]

[1]*Drug Discovery and Disease Research Laboratory, Shionogi & Co., Ltd., Osaka, Japan*
[2]*Department of Molecular Imaging and Radiotherapy, Graduate School of Pharmaceutical Sciences, Chiba University, Chiba, Japan*
[3]*Department of Biomarker Research and Development, Shionogi Co., Ltd., Osaka, Japan*

Abstract

Background: Chronic bacterial refractory infections remain critical health care issues. When studying chronic infections, it is important but currently difficult to evaluate bacterial behavior in live individual animals over time. Ubiquicidin (UBI) 29-41 labeled with ^{99m}Tc has been tested for the specific imaging of bacterial and fungal infections in various species. In this study, we investigated the feasibility of monitoring viable bacterial counts by single-photon emission computed tomography (SPECT) in the thigh muscle of mice infected with *Staphylococcus aureus* using two types of ^{99m}Tc-labeled 6-hydrazinonicotinic acid (HYNIC)-UBI 29-41.

Methods: ^{99m}Tc -HYNIC(Tricine)$_2$-UBI 29-41 and ^{99m}Tc -HYNIC(GH)$_2$-UBI 29-41 were synthesized, and their biodistribution was evaluated in normal mice. Each labeled peptide was injected into mice with *S. aureus* thigh infection after treatment with ciprofloxacin, and SPECT imaging was performed 2 h after the injection. The accumulation of labeled peptides at the thigh was assessed by SPECT, the number of viable bacteria was counted, and their correlation was evaluated. To evaluate bacteria regrowth, the same individual was administered the peptide twice and evaluated over time.

Results: The apparent molar activity of ^{99m}Tc-HYNIC(Tricine)$_2$-UBI 29-41 was 400 times higher than that of ^{99m}Tc-HYNIC(GH)$_2$-UBI 29-41. ^{99m}Tc-HYNIC(GH)$_2$-UBI 29-41 showed high organ distribution and was 2–10 times more distributed than ^{99m}Tc-HYNIC(Tricine)$_2$-UBI 29-41 in all organs at 0.5, 2, and 3 h after the injection of labeled peptides in normal mice. SPECT imaging revealed that the accumulation of labeled peptides in the bacterial infection site (left thigh) was higher than that in the non-infection site (right thigh) for both peptides. For ^{99m}Tc-HYNIC(GH)$_2$-UBI 29-41, the target-to-non-target ratio (T/NT) was 3.3 when the viable bacterial count was 10^8 colony-forming units (cfu)/thigh and decreased to 1.2 when the viable bacterial count was 10^3 cfu/thigh. For ^{99m}Tc-HYNIC(Tricine)$_2$-UBI 29-41, the T/NT ratio was significantly higher when the viable bacterial count was 10^8 cfu/thigh, with a value of 10.0. However, the T/NT ratio was 1.3 at 10^3 cfu/thigh, which is similar to the value for ^{99m}Tc-HYNIC(GH)$_2$-UBI 29-41 with the same bacterial count. A high correlation was found between the T/NT ratios of each labeled peptide and the viable bacterial count at the infection site. The correlation was confirmed under antibacterial treatment conditions.

Article Information

Article Type: Research
Article Number: JAMBR 153
Received Date: 19 January, 2022
Accepted Date: 16 February, 2022
Published Date: 23 February, 2022

***Corresponding author:** Yuri Nishiyama, Drug Discovery and Disease Research Laboratory, Shionogi & Co., Ltd., 3-1-1, Futaba-cho, Toyonaka, Osaka, 561-0825, Japan. Tel: +81-6-6331-7162; Email: yuri.nishiyama@shionogi.co.jp

Citation: Nishiyama Y, Uehara T, Okazaki K, Maki H, Abe K, et al. (2022) In Vivo Monitoring of Viable Bacteria by SPECT using 99mTc-HYNIC(GH)$_2$-UBI 29-41 and 99mTc-HYNIC(Tricine)$_2$-UBI 29-41 in Infected Mice. J Appl Microb Res. Vol: 5 Issu: 1 (01-07).

Bacterial regrowth after the cessation of antimicrobial agents was also monitored in live individual animals.

Conclusion: SPECT imaging with ^{99m}Tc-HYNIC-UBI 29-41 enabled the monitoring of viable bacterial counts in the range of 10^3–10^8 cfu/thigh in thigh-infected mice over time.

Keywords: Antimicrobial peptide, *Staphylococcus aureus*, Monitoring viable bacteria, Single-Photon Emission Computed Tomography (SPECT).

Abbreviations: Ubiquicidin (UBI), Single-Photon Emission Computed Tomography (SPECT).

Highlights

Monitoring viable bacteria *in vivo*

Monitoring individual animals over time

Correlation between peptide accumulation and viable bacterial counts

Introduction

Bacterial refractory infections continue to pose a serious global health concern. In addition to the development of antibacterial resistance, even though pathogenic bacteria remain sensitive to antibiotics, failed eradication of causative bacteria sometimes leads to relapse [1]. Both physiological and genetic changes in bacteria are thought to contribute to drug resistance or tolerance and persistence in chronic infections [2]. Some phenotypes are fastidious, as they are only maintained *in vivo* and somehow disappear once the bacteria are removed from the host.

Therefore, establishing a novel method to evaluate bacterial behavior during drug treatment in individual animals over time is essential to accelerate next-generation antibacterial drug discovery research. In conventional acute infection models, counting viable bacteria by euthanizing animals at each time point makes it difficult to monitor bacterial behavior in individual animals. In contrast, imaging technology provides a useful non-invasive method to evaluate bacterial behavior.

Two imaging methods show potential for evaluating infections: optical imaging and radioactivity-based methods. Van Oosten *et al.* reported the use of luciferase-engineered *Staphylococcus aureus* and fluorescently labeled vancomycin (vanco-800CW) in a mouse myositis model [3]. Bioluminescence was used to indicate the localization of *S. aureus* and allowed the overlap with vanco-800CW to be determined. Ning *et al.* demonstrated the *in vivo* detection of *Escherichia coli*, *S. aureus*, *Pseudomonas aeruginosa*, and *Bacillus subtilis* using maltodextrin-based imaging probes in a rat myositis model [4]. Tang *et al.* reported infection imaging using concanavalin A as a bacteria-targeting ligand, a nanoparticle carrier, and a near-infrared fluorescent dye in a mouse wound model [5]. Optical imaging is considered useful for detecting bacterial infections; however, it can only be used if the infection model is close to the surface, such as in subcutaneous and thigh infections. Furthermore, the optical imaging sensitivity of bacterial counts was reported to be approximately 10^5 cfu/thigh. Empirically, the number of viable bacteria is reduced to around 10^2–10^3 cfu/thigh following treatment with antibacterial agents [3-5]. However, if relapse occurs when treatment is discontinued, optical imaging is considered to have insufficient sensitivity to monitor the bacteria.

The other imaging technology is based on radioactivity. Radioactivity-based methods can be used to evaluate deep infections, such as lung infections, in addition to those near the surface, and they generally have higher sensitivity than optical imaging. Therefore, we selected single-photon emission computed tomography (SPECT) with ^{99m}Tc-labeled probes to monitor the same animal using radioactivity.

Several radiolabeled agents, such as antibodies, antibiotics, and peptides, have been evaluated for imaging infections [6]. Among them, ubiquicidin (UBI) 29-41 was selected as the probe to be examined in this study. UBI 29-41 is one of the infection probes used clinically that binds to a broad spectrum of Gram-positive and Gram-negative bacteria and fungi [7]. UBI 29-41 is a cationic human antimicrobial peptide fragment with six positively charged residues (5 Arg + 1 Lys) that accumulates at the negatively charged surfaces of microorganisms. Nibbering *et al.* reported *in vivo* studies using UBI 29-41 in mice and rats infected with *S. aureus* [8]. They monitored the efficacy of antibiotics and reported a high correlation between the accumulation of UBI 29-41 at the infection site and the dose of antibiotics administered.

It has been reported that the nature of the coligand affects the biodistribution of ^{99m}Tc-labeled 6-hydrazinonicotinic acid (HYNIC)-chemotactic peptides [9]. In this report, we synthesized two types of labeled UBI 29-41 with α-D-glucoheptonic acid (GH) and tricine as coligands. Using these two labeled peptides, we evaluated the feasibility of *in vivo* monitoring of viable bacterial counts by SPECT.

Materials and Methods

Antibiotics and synthetic antimicrobial peptides

Ciprofloxacin (CPFX; hydrochloride, ≥ 98% activity) was purchased from LKT Laboratories, Inc. (MN, USA). Cyclophosphamide (CY; hydrate, 94% activity) was purchased from Shionogi & Co., Ltd. (Osaka, Japan). Brain-Heart Infusion (BHI) broth and agar were purchased from BD. (NJ, USA) UBI 29-41 denotes TGRAKRRMQYNRR (1693 Da). HYNIC-UBI 29-41 was synthesized at Toray Research Center (Tokyo, Japan, Figure 1).

Labeling procedure and quality control

^{99m}Tc-HYNIC$(GH)_2$-UBI 29-41 was labeled as follows: 2 mg of the GH kit (freeze-dried GH 2 mg and $SnCl_2/2H_2O$ 1.2 μg) was dissolved in 1 mL of $^{99m}TcO_4^-$ (185 MBq/mL, Nihon Medi-Physics Co. Ltd.), and the sample was incubated for 10

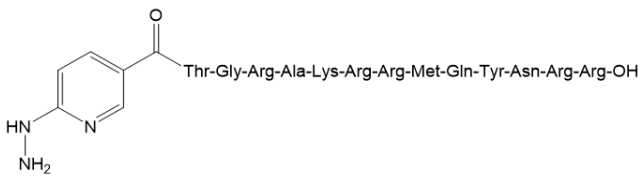

Figure 1: Structural formula of HYNIC-UBI 29-41.

min at room temperature to synthesize ^{99m}Tc-GH. Then, 200 µL of the ^{99m}Tc-GH solution and 200 µL of 400 µM HYNIC-UBI aqueous solution were mixed and incubated for 60 min at room temperature. ^{99m}Tc-HYNIC(Tricine)$_2$-UBI 29-41 was labeled as follows: 125 µL of $^{99m}TcO_4^-$ was mixed with 125 µL of 40 mg/mL tricine in 10 mM acetate buffer (pH 4). Then, 10 µL of 25 µM HYNIC-UBI aqueous solution and 6 µL of 1 mg/mL $SnCl_2/2H_2O$ in 0.1 N HCl were added, and the sample was incubated for 10 min at 90°C [10]. In both labeled reactions, the amount of HYNIC-UBI was sufficient to bind all ^{99m}Tc. Following labeling, each reaction mixture was analyzed by reverse-phase high-performance liquid chromatography (RP-HPLC). The sample was applied to an XBridge® C18 5-µm column (4.6 × 150 mm, Waters) attached to a chromatograph equipped with an online UV detector set at 254 nm and a NaI (Tl) crystal gamma detection system (Gabi star, Raytest, Straubenhardt, Germany). ^{99m}Tc-HYNIC(GH)$_2$-UBI 29-41 was detected using a linear gradient of two eluents at a flow rate of 1.2 mL/min: 0.1% (v/v) trifluoroacetic acid (TFA)/water (solvent A) and 0.1% TFA/acetonitrile (solvent B). The gradient was applied as follows: 95%–20% A in 15 min and 95% A for 5 min. ^{99m}Tc-HYNIC(Tricine)$_2$-UBI 29-41 was detected using a linear gradient of two eluents at a flow rate of 1.0 mL/min: 0.01% (v/v) TFA/water (solvent A) and 0.01% TFA/acetonitrile (solvent B). The gradient was applied as follows: 95%–70% A in 20 min and 95% A for 5 min.

Microorganism

S. aureus 25923 (American Type Culture Collection) susceptible to CPFX (minimum inhibitory concentration < 1 µg/mL) was used. *S. aureus* 25923 was cultured on Brain–Heart Infusion Agar for 24 h at 37°C. The colony suspension was washed, counted by optical density, and used in the *in vitro* binding assay. The viable cell count was also determined by plating on Brain–Heart Infusion Agar. For the *in vivo* assay, a stock solution of *S. aureus* 25923 stored at −80°C was used.

In Vitro binding to *S. aureus*

Ten microliters of the preparation containing each labeled peptide and 10 µL of suspension containing 5×10^{10} cfu/mL *S. aureus* were added to 80 µL of a binding buffer (20 mM phosphate buffered saline containing 0.01% Tween80 and 5 mM acetic acid, pH=5). For the serum conditions, 10 µL of mouse serum were added instead of 10 µL of the binding buffer. The suspensions were gently mixed using a vortex mixer and incubated at 37°C for 1 h. After incubation, the tubes were centrifuged at 5000 ×g for 10 min. The supernatant was removed, and the pellet was resuspended in 100 µL of binding buffer and re-centrifuged at 5000 ×g for 10 min. The supernatant was removed, and the radioactivity of the pellet was counted using a γ-counter. The radioactivity associated with the bacteria pellet was expressed as a percentage of the total ^{99m}Tc activity added.

Animals

All procedures for animal studies were approved by the Institutional Animal Care and Use Committee of Shionogi & Co., Ltd. (Osaka, Japan). Specific-pathogen-free male ICR mice (CLEA Japan Inc., 5 weeks old) were used in the infection and SPECT studies.

Biodistribution

A 0.2-mL solution containing 30 kBq of ^{99m}Tc-HYNIC(Tricine)$_2$-UBI 29-41 or 10 kBq of ^{99m}Tc-HYNIC(GH)$_2$-UBI 29-41 was administered via the tail vein of mice. Animals were euthanized by exsanguination, and the thoracic cavity was opened at 0.5, 2, and 3 h post injection. Organs were excised and weighed, and the activity of probes was counted using a γ-counter. Organ uptake was calculated as a percentage of the injected dose per gram of wet tissue (%ID/organ, Table 1).

Treatment of animal infections with antibacterial agents

Normal and immunosuppressed mice were used. To generate immunosuppressed mice, CY was injected by intraperitoneal administration at 4 days and 1 day before infection. Mice were anesthetized with isoflurane, and 6.0×10^6–2.0×10^7 cfu of bacteria in 0.1 mL saline were aseptically injected into the left thigh muscle of each mouse. The antimicrobial procedures (original) were as follows: mice were subcutaneously administered 10–100 mg/kg of CPFX once a day or three times a day for 2 days after infection (Figure 2A, B). In experiments to monitor regrowth, mice were administered CPFX only once 2 h after infection (Figure 2C).

SPECT imaging

At 46 h after infection, 0.2 mL of a solution containing 10–30 MBq of each labeled peptide was administered via the tail vein of mice (Figure 2A, B). In experiments for monitoring regrowth, the labeled peptide was administered at 22 h and 70 h after infection (Figure 2C).

The accumulation of each labeled peptide in the bacteria-infected site in mice was assessed by SPECT/CT (Triumph

Labeled peptide	Time after injection	Lung	Liver	Kidney	Left thigh	Blood
GH	30 min	4.07 ± 0.50	5.07 ± 0.51	46.16 ± 1.46	1.41 ± 0.18	3.43 ± 0.11
	2 hr	3.55 ± 0.43	7.37 ± 0.77	56.53 ± 9.20	1.17 ± 0.25	2.41 ± 0.29
	3 hr	3.75 ± 0.24	8.18 ± 0.07	65.45 ± 4.33	1.11 ± 0.24	2.34 ± 0.11
Tricine	30 min	1.77 ± 0.16*	2.11 ± 0.12*	83.89 ± 5.83*	0.84 ± 0.06*	2.01 ± 0.19*
	2 hr	0.55 ± 0.04*	1.96 ± 0.02*	84.88 ± 16.08	0.22 ± 0.01*	0.40 ± 0.05*
	3 hr	0.36 ± 0.03*	2.08 ± 0.26*	73.07 ± 9.81	0.18 ± 0.03*	0.22 ± 0.03*

Expressed as % injected dose per gram. Each value represents the mean (SD) for three animals at each interval. *Values that were significantly ($P<0.05$) different compared with GH.

Table 1: Biodistribution of ^{99m}Tc-HYNIC(Tricine)$_2$-UBI 29-41 and ^{99m}Tc-HYNIC(GH)$_2$-UBI 29-41 in mice

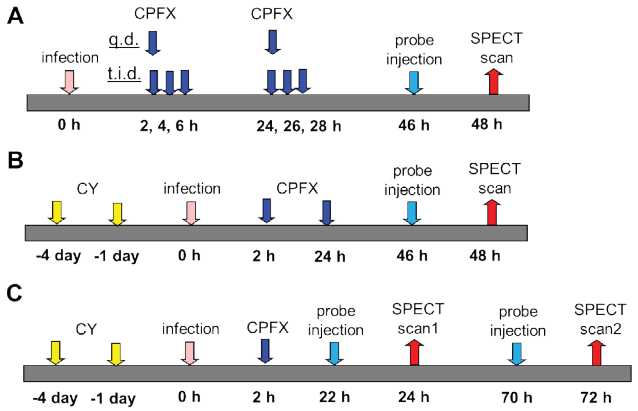

Figure 2: Schematic diagram of the experimental protocol infected with *S. aureus* in normal mice (A) in immunosuppressed mice (B) at monitoring for regrowth (C).

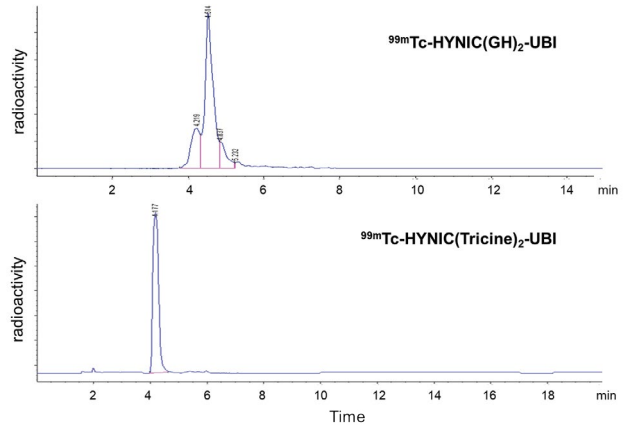

Figure 3: Typical HPLC radioactivity profiles of ^{99m}Tc-HYNIC(GH)$_2$-UBI and ^{99m}Tc-HYNIC(Tricine)$_2$-UBI.

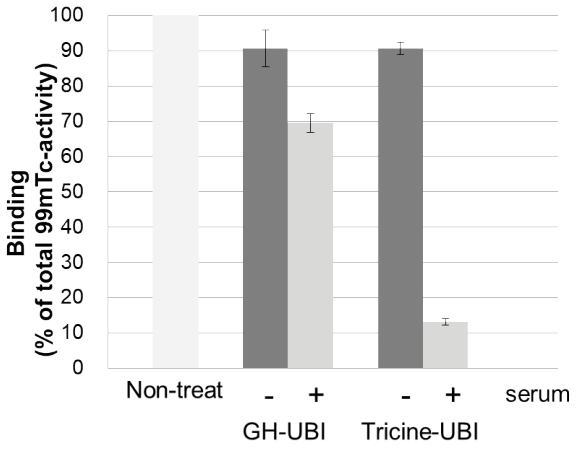

Figure 4: *In vitro* bacterial binding of ^{99m}Tc-HYNIC(GH)$_2$-UBI 29-41 and ^{99m}Tc-HYNIC(Tricine)$_2$-UBI 29-41 to *S. aureus*. Results are expressed as the mean ± SD for three tests.

II SPECT 2H/XO SRI CT, TriFoil Imaging). Two hours after the labeled peptide injection, mice were anesthetized with isoflurane. Mice were then arranged lying face down on a SPECT/CT bed with both hind legs spread out and fixed with surgical tape. Whole body images were acquired under the following conditions: energy window, 20% at 140 keV; projection limit, 20 s; projection count, 64; and rotation angle, 360 degrees. The total time for actual imaging was only ~20 min. After whole body imaging, the mice were euthanized, and the infected (left) and normal (right) legs were extracted. Leg-only images were then acquired using the same conditions. For image processing, adjusted regions of interest were drawn over the entire infected muscle (target [T]) and contralateral muscle (nontarget [NT]). The accumulation of each labeled peptide at the infection site was expressed as the ratio of the counts in the target and nontarget muscles (T/NT).

Determining the number of viable bacteria

After SPECT imaging, the entire infected thigh muscles were removed and individually homogenized in Mueller–Hinton broth. Serial dilutions of the thigh homogenate were plated on Brain–Heart Infusion Agar. The plates were then incubated for 24 h at 37°C, and the numbers of colonies were counted. The viable bacterial counts in thigh (log10 CFU/thigh) were calculated from the number of colony in the plate.

Statistical Analysis

The differences between log cfu before and after treatment with CPFX in mice were evaluated using the Student's t-test. The P values were calculated, and statistical significance was accepted within 95% confidence limits by SAS® Version 9.4. All results were reported as means and SD. The Pearson correlation coefficient (r) was used to assess the correlation between the labeled peptide accumulation and the viable bacterial count.

Results

Labeling and quality control

RP-HPLC analysis of ^{99m}Tc-HYNIC(GH)$_2$-UBI 29-41 showed two major peaks (4.2 and 4.5 min), and that of ^{99m}Tc-HYNIC(Tricine)$_2$-UBI 29-41 showed a single peak (4.2 min, Figure 3). Leading and trailing shoulders were detected for both peptides; however, a previous report indicated that derivatives with GH and tricine as coligands existed in many isomeric forms [11]. In both labeled reactions, the amount of HYNIC-UBI was sufficient to bind all ^{99m}Tc. The radiochemical purity was 91±9% (n=8) for ^{99m}Tc-HYNIC(GH)$_2$-UBI 29-41 and 100% (n=8) for ^{99m}Tc-HYNIC(Tricine)$_2$-UBI 29-41. Each labeled peptide was administrated without purification. The apparent molar activity of ^{99m}Tc-HYNIC(GH)$_2$-UBI 29-41 was 0.85±0.085 GBq/μmol (n=8), and that of ^{99m}Tc-HYNIC(Tricine)$_2$-UBI 29-41 was 389 GBq/μmol (n=8). It was confirmed that the stability of each labeled peptide had decreased by only a few percent at 2 h after administration to the second animal.

In Vitro binding to *S. aureus*

The binding of ^{99m}Tc-HYNIC(GH)$_2$-UBI 29-41 to *S. aureus* (5×10^8 cfu/tube) without serum was 90.7±5.2% of the total ^{99m}Tc activity, and in the presence of serum, the binding was 69.5±2.7%. The binding of ^{99m}Tc-HYNIC(Tricine)$_2$-UBI 29-41

was 90.7±1.7% without serum and decreased to 13.2±1.0% in the presence of serum (Figure 4).

Biodistribution

The biodistributions of ^{99m}Tc-HYNIC(GH)$_2$-UBI 29-41 and ^{99m}Tc-HYNIC(Tricine)$_2$-UBI 29-41 in normal mice at 0.5, 2, and 3 h are summarized in table 1. The data showed that the highest concentrations of radioactivity were measured in the kidney for both peptides. The accumulation of ^{99m}Tc-HYNIC(GH)$_2$-UBI 29-41 in the kidney increased over time, whereas ^{99m}Tc-HYNIC(Tricine)$_2$-UBI 29-41 decreased. ^{99m}Tc-HYNIC(GH)$_2$-UBI 29-41 showed high organ distribution and was 2–10 times more distributed than ^{99m}Tc-HYNIC(Tricine)$_2$-UBI 29-41 in all organs at all time points. This difference in organ distribution is attributed to the difference in coligands. The activity at the infection site in the thigh showed no further increase after 2 h; therefore, the SPECT images were acquired 2 h after peptide injection.

Effect of antibiotic administration

To evaluate the correlation between the labeled peptide accumulation and the viable bacterial count, it was necessary to establish various viable bacterial counts. In addition to the untreated (control) group, 2-day treatment with 10–100 mg/kg of CPFX was administered to mice. As a result, viable bacterial counts in the range of 10^3–10^8 cfu/thigh were established (Figure 5). This range was considered sufficient to evaluate treatment with antibiotics in a chronic infection model.

Detection of labeled peptide accumulation at the infection site using SPECT

The bacterial infection site was imaged 2 h after the injection of each labeled peptide. Of the many tests performed with 10^3–10^8 cfu/thigh, representative images for each labeled peptide in *S. aureus*-infected mice are shown in figure 6. For ^{99m}Tc-HYNIC(GH)$_2$-UBI 29-41, the T/NT ratio was 3.3 when the viable bacterial count was 10^8 cfu/thigh and decreased to 1.2 when the viable bacterial count was 10^3 cfu/thigh. For ^{99m}Tc-HYNIC(Tricine)$_2$-UBI 29-41, the T/NT ratio was significantly higher when the viable bacterial count was 10^8 cfu/thigh, with a value of 10.0. However, the T/NT ratio was 1.3 at 10^3 cfu/thigh, which is similar to the value for ^{99m}Tc-HYNIC(GH)$_2$-UBI 29-41 with the same bacterial count.

The correlations between the accumulation of each labeled peptide and the viable counts of bacterial are shown in figure 7. The accumulation of each labeled peptide showed a high correlation with the viable bacterial count: r=0.906 and P=0.002 for ^{99m}Tc-HYNIC(GH)$_2$-UBI 29-41; r=0.857 and P=0.001 for ^{99m}Tc-HYNIC(Tricine)$_2$-UBI 29-41.

Monitoring for regrowth by SPECT

The mice were treated with CPFX 2 h after infection and first imaged at 24 h after infection when the bacteria had decreased. Afterward, individual mice were re-imaged at 72 h after infection when the remaining bacteria had regrown (Figure 2C). In the CPFX treatment group, the viable bacterial count was 10^5 cfu/thigh at 24 h after infection but increased to 10^8 cfu/thigh at 72 h. The T/NT ratio value increased from 1.8 at 24 h to 2.8 at 72 h after treatment with CPFX (Figure 8).

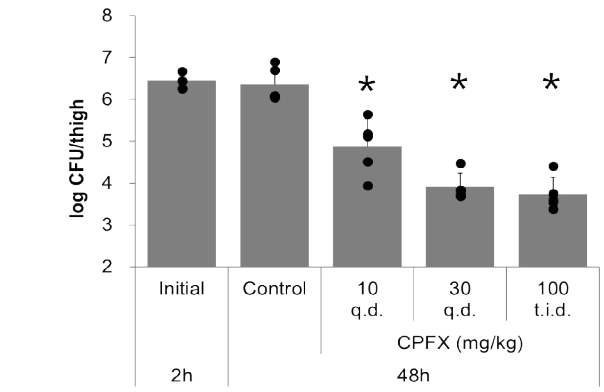

Figure 5: Viable bacterial count in thigh infected with *S. aureus* for normal mice treated with CPFX for 2 days. Results are expressed as the mean ± SD for three animals. *Values that were significantly (P < 0.05) different to the control.

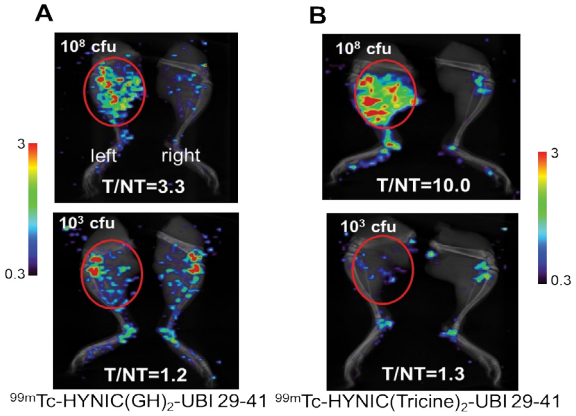

Figure 6: SPECT images of [A] ^{99m}Tc-HYNIC(GH)$_2$-UBI 29-41(10MBq) in normal mice [B] ^{99m}Tc-HYNIC(Tricine)$_2$-UBI 29-41(30MBq) in immunosuppressed mice. Mice were infected in the left thigh (red circle) with *S. aureus*, acquired 2 h after the administration.

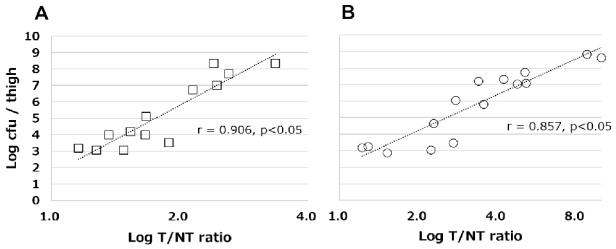

Figure 7: Correlation between viable *S. aureus* counts and the accumulation of [A] ^{99m}Tc-HYNIC(GH)$_2$-UBI 29-41 in normal and immunosuppressed mice (square) [B] ^{99m}Tc-HYNIC(Tricine)$_2$-UBI 29-41 in immunosuppressed mice (circle), expressed as the target-to-non-target(T/NT) ratio.

Discussion

The biodistributions of ^{99m}Tc-HYNIC(GH)$_2$-UBI 29-41 and ^{99m}Tc-HYNIC(Tricine)$_2$-UBI 29-41 in normal mice both showed high renal excretion. Welling MM *et al.* reported that ^{99m}Tc-HYNIC(Tricine)$_2$-UBI 29-41 showed rapid elimination mainly through the kidneys and poor distribution in all organs [12]. The clearance of ^{99m}Tc-HYNIC(GH)$_2$-UBI 29-41 was slower than that of ^{99m}Tc-HYNIC(Tricine)$_2$-UBI 29-

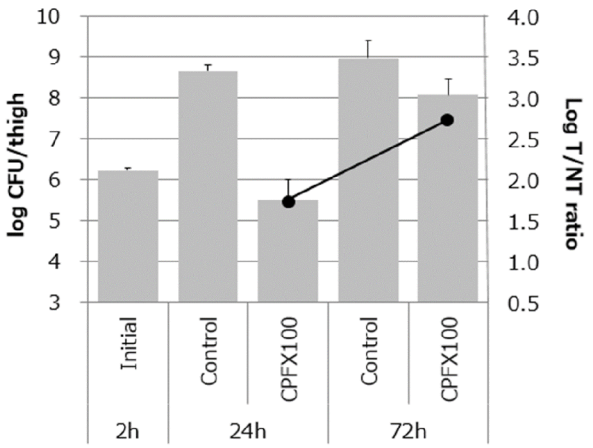

Figure 8: Left axis (bar graph): Viable bacterial count in thigh infected with *S. aureus* for immunosuppressed mice treated with CPFX. Results are expressed as the mean ± SD for three animals. Right axis (line graph): The accumulation of ^{99m}Tc-HYNIC(GH)$_2$-UBI in the left thigh. Results are expressed as the mean for two animals.

41, and the distribution of ^{99m}Tc-HYNIC(GH)$_2$-UBI 29-41 in organs was higher than that of the other peptide. The binding of ^{99m}Tc-HYNIC(Tricine)$_2$-UBI 29-41 was influenced by the presence of serum (Figure 4). Several research groups have reported that small biomolecules labeled with tricine as a coligand were unstable and existed as multiple species in solution and that they may react with the imidazole group of histidine residues in circulating blood proteins, such as albumin [13,14]. Therefore, the low organ distribution of ^{99m}Tc-HYNIC(Tricine)$_2$-UBI 29-41 is attributed to similar interactions. In addition, because ^{99m}Tc-HYNIC(Tricine)$_2$-UBI 29-41 is less hydrophobic than ^{99m}Tc-HYNIC(GH)$_2$-UBI 29-41, it shows less non-specific binding to organs.

Next, we aimed to quantify the viable bacteria by measuring the amount of labeled peptide accumulated in the bacteria using SPECT. To this end, we investigated the correlation between the labeled peptide accumulation and the viable bacterial counts. To the best of our knowledge, this correlation has only been investigated by Lupetti *et al.* using ^{99m}Tc-labeled fluconazole with *Candida albicans* at 10^6–10^8 cfu/g tissue (about 10^5–10^7 cfu/thigh), and a high correlation was observed [15]. In this study, we used a dynamic range of bacterial counts from 10^3–10^8 cfu/thigh. Empirically the number of viable bacteria is reduced to around 10^2–10^3 cfu/thigh following treatment with antibacterial agents, the lower limit was set at 10^3 cfu/thigh. To achieve this bacterial count, mice were treated with CPFX. The bacterial count reached a minimum of 10^4 cfu/thigh on the first day of treatment and reached the target of 10^3 cfu/thigh on the second day of treatment (Figure 5).

The accumulation of each labeled peptide was evaluated at high bacterial counts (10^7–10^8 cfu/thigh) using SPECT. The T/NT ratio of ^{99m}Tc-HYNIC(GH)$_2$-UBI 29-41 was 2.4, and that of ^{99m}Tc-HYNIC(Tricine)$_2$-UBI 29-41 was 10.0 (Figure 6). We then investigated peptide accumulation at the detection target of 10^3 cfu/thigh using the same method and determined T/NT ratios of 1.2 and 1.3 for ^{99m}Tc-HYNIC(GH)$_2$-UBI 29-41 and ^{99m}Tc-HYNIC(Tricine)$_2$-UBI 29-41, respectively. The T/NT ratio range of ^{99m}Tc-HYNIC(GH)$_2$-UBI 29-41 was 1.2–3.3, and that of ^{99m}Tc-HYNIC(Tricine)$_2$-UBI 29-41 was 1.3–10.0.

This difference in the T/NT ratio range is thought to be due to variations in the biodistributions of each peptide and their binding activity to bacteria. ^{99m}Tc-HYNIC(Tricine)$_2$-UBI 29-41 exhibited less non-specific binding to organs than ^{99m}Tc-HYNIC(GH)$_2$-UBI 29-41 (Table 1), which is one of the factors indicating a high T/NT ratio at a high bacterial count. However, due to the lower accumulation of ^{99m}Tc-HYNIC(Tricine)$_2$-UBI 29-41 than ^{99m}Tc-HYNIC(GH)$_2$-UBI 29-41, the injection dose for ^{99m}Tc-HYNIC(Tricine)$_2$-UBI 29-41 had to be higher to be detected by SPECT. In this study, both peptides with different properties could be detected by SPECT, but it was necessary to adjust the injection dose for each labeled peptide according to the lower limit of quantification of SPECT. Based on this thigh infection system, ^{99m}Tc-HYNIC(Tricine)$_2$-UBI 29-41 is more suitable for quantifying bacteria than ^{99m}Tc-HYNIC(GH)$_2$-UBI 29-41.

In this report, it was possible to monitor decreases in the number of bacteria with antibacterial agents. This suggests that bacteria killed by antibacterial agents are eliminated from the site of infection by the immune system. Moreover, it has been reported that UBI does not accumulate in sterile inflammation, and its accumulation at the infected site is thought to occur only in viable bacteria [16,17].

This study determined that SPECT imaging with ^{99m}Tc-HYNIC-UBI29-41 is a useful method to quantify viable bacteria in the range 10^3–10^8 cfu/thigh by measuring the accumulation of labeled peptides. Furthermore, even with continuous SPECT imaging in individual mice, the accumulation of the labeled peptide showed a high correlation with the viable bacterial count.

In this study, we examined one bacterial species and model. Therefore, we aim to study other bacterial species and models for research on bacterial refractory infections involving persisters and biofilms in the future.

Conclusion

SPECT imaging can be used to quantify viable bacterial counts ranging from 10^3 to 10^8 cfu/thigh by measuring the accumulation of labeled antimicrobial peptides. This approach enables the monitoring of viable bacterial counts in live individual animals over time, which is required for the investigation of chronic bacterial refractory infections.

Acknowledgment

We thank Yumi Sato for helping with ^{99m}Tc labeling and Masaaki Izawa for establishing the mouse infection model.

Funding

This research did not receive any specific grant from funding agencies in the public, commercial, or not-for-profit sectors.

Competing Interests

The authors declare that they have no conflicts of interest.

References

1. ReAct facts (2012) Burden of antibiotic resistance.
2. Maisonneuve E, Gerdes K (2014) Molecular mechanisms underlying bacterial persisters. Cell 157: 539-548.
3. Van Oosten M, Schafer T, Gazendam JAC (2013) Real-time in vivo imaging of invasive- and biomaterial-associated bacterial infections using fluorescently labelled vancomycin. Nat Commun 4: 2584.
4. Ning X, Lee S, Wang Z (2011) Maltodextrin-based imaging probes detect bacteria in vivo with high sensitivity and specificity. Nat Mater 10: 602-607.
5. Tang E, Nair A, Baker DW (2014) In vivo imaging of infection using a bacteria-targeting optical nanoprobe. J Biomed Nanotechnol 10: 856-863.
6. Van Oosten M, Hahn M, Crane LM (2015) Targeted imaging of bacterial infections: advances, hurdles and hopes. FEMS Microbiology Reviews 39: 892-916.
7. Sathekge M, Garcia-Perez O, Paez D (2018) Molecular imaging in musculoskeletal infections with ^{99m}Tc-UBI 29-41 SPECT/CT. Ann Nucl Med 32: 54-59.
8. Nibbering PH, Welling MM, Paulusma-Annema A (2004) ^{99m}Tc-Labeled UBI 29-41 peptide for monitoring the efficacy of antibacterial agents in mice infected with Staphylococcus aureus. J Nucl Med 45: 321-326.
9. Babich JW, Fischman AJ (1995) Effect of "co-ligand" on the biodistribution of ^{99m}Tc-labeled hydrazine nicotinic acid derivatized chemotactic peptides. Nucl Med Biol 22: 25-30.
10. Welling MM, Korsak A, Gorska B (2005) Kit with technetium-99m labelled antimicrobial peptide UBI 29-41 for specific infection detection. J Label Compd Radiopharm 48: 683-691.
11. Edwards DS, Liu S, Ziegler MC (1999) RP463: A stabilized technetium-99m complex of a hydrazino nicotinamide derivatized chemotactic peptide for infection imaging. Bioconjug Chem 10: 884-891.
12. Welling MM, Visentin R, Feitsma HIJ (2004) Infection detection in mice using ^{99m}Tc-labeled HYNIC and N_2S_2 chelate conjugated to the antimicrobial peptide UBI 29-41. Nucl Med Biol 31: 503-509.
13. Meszaros LK, Dose A, Biagini SCG (2010) Hydrazinonicotinic acid (HYNIC) – coordination chemistry and applications in radiopharmaceutical chemistry. Inorganica Chim Acta 363: 1059-1069.
14. Purohit A, Liu S, Ellars CE (2004) Pyridine-containing 6-hydrazinonicotinamide derivatives as potential bifunctional chelators for ^{99m}Tc-labeling of small biomolecules. Bioconjug Chem15: 728-737.
15. Lupetti A, Welling MM, Mazzi U (2002) Technetium-99m labelled fluconazole and antimicrobial peptides for imaging of Candida albicans and Aspergillus fumigatus infections. Eur J Nucl Med 29:674-679.
16. Akhtar MS, Iqbal J, Khan MA (2004) ^{99m}Tc-labeled antimicrobial peptide ubiquicidin (29-41) accumulates less in *Escherichia coli* infection than in *Staphylococcus aureus* infection. J Nucl Med 45: 849-856.
17. Gandomkar M, Najafi R, Mazidi M (2008) New peptide based freeze-dried kit [^{99m}Tc-HYNIC]-UBI 29-41 as a human specific infection imaging agent. Iran J Nucl Med 16: 25-30.

Citation: Nishiyama Y, Uehara T, Okazaki K, Maki H, Abe K, et al. (2022) In Vivo Monitoring of Viable Bacteria by SPECT using 99mTc-HYNIC$(GH)_2$-UBI 29-41 and 99mTc-HYNIC$(Tricine)_2$-UBI 29-41 in Infected Mice. J Appl Microb Res. Vol: 5 Issu: 1 (01-07).